Membrane and Water Treatment, *Vol. 15, No. 3 (2024) 131-137*
https://doi.org/10.12989/mwt.2024.15.3.131

Fabrication of carboxymethyl functionalized Euryale ferox starch-based hydrogel for efficient removal of methylene blue

Xue-Li Liu*[1], Zhong-Zhu Hu[1], Ya-Li Sun[1] and Chun-Feng Zhu**[2]

[1]*College of Material and Chemical Engineering, Chuzhou University, Anhui 239012, China*
[2]*Department of Pharmacy, Lu'an Hospital of Traditional Chinese Medicine, 237000, China*

(Received May 28, 2024, Revised June 28, 2024, Accepted August 1, 2024)

Abstract. *Euryale ferox Salisb*. is an important plant resource and valuable tonic in traditional Chinese medicine. The seed of *Euryale ferox Salisb.* is rich in starch. There are few reports of modification and functional properties of Euryale ferox starch. In present study, the *Euryale ferox* starch was extracted, carboxymethyl etherified starches were synthesized, the starch-based hydrogels were prepared, and adsorptive properties were investigated. The results of investigation showed that carboxymethyl etherified *Euryale ferox* starch-based adsorbent has the potential for methylene blue removal. Therefore, *Euryale ferox* starch has an appealing application prospect in adsorption for scavenging dyes from real complex waste liquid.
Keywords: adsorption application; chemical modification; Euryale ferox starch;

1. Introduction

Euryale ferox Salisb. is an annual large-scale aquatic herb belonging to the genera Euryale of the family Nymphaeaceae and the seeds of Euryale ferox, known as *Qianshi*, *Jitoumi*, and *Gorgon nut*, are widely used in traditional Chinese medicine and food because of their good taste and huge yield (Jha *et al*. 2018, Khadatkar *et al*. 2020, Jiang *et al*. 2023). The deep processing of *Euryale ferox* has great development potential and market prospects. The most important nutrient substance in Euryale ferox is carbohydrate, of which the starch content is higher than 70% (Zhang *et al*. 2023). *Euryale ferox* kernel starch has yet to be harnessed, despite its high starch content. At present, the researches on *Euryale ferox* are mainly focused on its nutrition and physiological activity, and the researches on *Euryale ferox* starch are concentrated in physicochemical properties (Yang *et al*. 2021, Zhao *et al*. 2022, Wang *et al*. 2023), digestion properties (Zhang *et al*. 2023, Biswas *et al*. 2020, Maibam *et al*. 2023), and application in foods (Devi *et al*. 2022). However, to the best of our knowledge, few studies have been reported about the functional side for non-food-based applications of kernel starch from *Euryale ferox* seeds, but there have been two previous studies investigating physicochemical properties of acetylated (Bhat *et al*. 2023) and octenyl succinic anhydride (Shweta *et al*. 2021) *Euryale ferox* starch. Therefore, we conducted the present research to investigate the starch modification and functional properties of *Euryale ferox* starch.

Starch has been extensively studied and discussed in literatures. Physicochemical properties of starch determined its application in food and nonfood industries. However, starch has limited applications in its natural condition, so it may lack the properties required for a particular processing method with chemical, physical, or biological treatments (Zia-ud-Din *et al*. 2015). After suitable modification, the scale-inhibition performance of starch-based materials could be evidently improved. Among them, carboxymethyl starch (CMS) is one of simplest starch derivatives, which contains abundant hydroxyl and carboxyl groups on the chain backbone. CMS-based polymer, with the advantages of nontoxic, wide source, and excellent biodegradability, has been studied in the field of polluted wastewater treatment and proved to be the most abundant biopolymers (Musarurwa *et al*. 2020). However, due to the poor mechanical and physical properties, it is necessary to be cross-linked with other materials to improve their mechanical properties (Zdanowicz *et al*. 2014).

Hydrogels have a three-dimensional network structure and hydrophilic groups, which can preserve a large amount of water without being soluble in water (Chen *et al*. 2022). The hydrophilic groups of network structure, such as hydroxyl groups, sulphonic groups, and amide groups, can be chelated with several kinds of heavy metal ion effectively (Guo *et al*. 2020). Hydrogels can be divided into synthetic and natural hydrogels in terms of synthetic raw materials. Correspondingly, starch can be used to prepare natural hydrogel, has great value to technical study and has good prospects for application.

As a result, the goal of this study was to extract the starch from *Euryale ferox* seeds, and explore its functional side for other food and non-food-based applications. In this context, the present work was designed to modify and characterize starch-based hydrogel by different level of carboxymethylation. Secondly, the modified particles were utilized to the adsorption of Methylene Blue (MB). Finally,

*Corresponding author, Ph.D.,
E-mail: n_xueli@163.com
**Co-corresponding author, Ph.D.,
E-mail: zcf_1217@163.com

Copyright © 2024 Techno-Press, Ltd.

ISSN: 2005-8624 (Print), 2092-7037 (Online)

the adsorption kinetics and adsorption isotherms of MB on the composite film were also investigated. The research on environmentally friendly materials applied in improving adsorption capacity has profound significance in environmental pollution management.

2. Materials and methods

2.1 Materials

Euryale ferox seeds was obtained from MinNong traditional Chinese medicine Co., LTD (Gansu, China). Microcrystalline cellulose (MCC) was purchased from Zhejiang YiNuo Biotechnology Co., LTD (Zhejiang, China). Other chemicals and reagents were analytical grade.

2.2 Extraction of native starch (NS)

The NS was extracted from *Euryale ferox* seeds by ethanol-alkali extraction based on the method described previously (Huang *et al*. 2016), with some modifications. The *Euryale ferox* seeds experienced several processes of cleaning, size reduction, soaking, and drying. Among them, the seeds were comminuted to powders and sieved with 200mesh sifters. Dried powders were extracted repeatedly by ethanol for 24 h at 25℃ until the liquid extract became light or colorless. Then the settled starch solid was dispersed and stirred in sodium hydroxide solution (0.1%, w/w) over a hot water bath at 50℃ for 1h. Combined the centrifugation and washed with deionized water three times, the purified native starch was obtained and dried at 60℃ under a vacuum for 24h. Crushed the starch and sieved with 200mesh sifters for further analyses.

2.3 Carboxymethylation of native starch (CMNS)

CMNS was synthesized by using the monochloroacetic acid (MCA) as etherifying agent. Set the molar ratios of MCA to NS to 0.6, 1.1, and 2.0. Meanwhile, keep the molar ratio of NaOH to MCA to 2.1. For example, 5.4g of NS and 1.68g of NaOH were added into a 34 mL of 80% ethanol solution, then stirring for 1 h in a water bath at 30 °C. Dissolved the 1.8g MCA in the 80% ethanol solution (17mL) which was dropwise added into the reaction phase and kept the reaction at 50 °C for 4h. The mixture was adjusted to neutral pH with hydrochloric acid aqueous solution, and then deposited in 95% ethanol. The obtained product was dried in an oven at 60 °C for 48 h. The products were marked as CMNS-0.6, CMNS-1.1, CMNS-2.0. The DS of CMNSs were analyzed by the method of complexometric titration (Wilpiszewska *et al*. 2015). The MSs obtained for the CMNS were 0.129, 0.571, 0.749, respectively.

2.4 Preparation of Starch-based hydrogel

The starch-based hydrogel was prepared according to the following procedure. 1.0 g of CMNS was transferred to a 100 mL breaker and 10 mL deionized water was added. The Slurry was heated in a boiling bath for 10 min and then cooled to room temperature. 30 mL suspension of MCC (0.5 g, well-diversified) was added and stirred in well. 5 mL of AA was measured in another 100 mL breaker, the neutralization was adjusted to 60% with aqueous NaOH (15wt%), and 0.2 g cross-linking agent of N, N'-methylenebisacrylamide (NMBA) was added, then the two breakers were mixed and dissolved. The temperature rises steadily to 75℃ upon including the activator ammonium persulfate (APS, 0.06g), which is maintained for three hours. The hydrogel was washed with deionized water to get rid of extra agents, and then washed with ethanol to remove the water from the hydrogel, Finally, for additional testing, the dried samples were crushed. The products of CMNS/AA hydrogel were marked as HCMNS.

2.5 Adsorption experiments

MB solution was prepared at room temperature in advance. Then, a series of desired concentration of MB solutions were obtained through dilution of the stock solution. Adsorption experiments were launched in thermostatic shaker (THZ-82B, Shanghai Keheng Industrial Development Co., LTD., China) with 180rpm. The simulated solutions of MB with concentrations of 100 mg/L. Experimental system contained a certain amount (0.02g) of starch-based hydrogel dispersed in 100mL MB at temperature of 298 K until adsorption equilibrium. The concentrations of MB for all samples after the adsorption experiments were measured using a UV-Visible spectrophotometer (UV-5100, Shanghai Yuanxi Apparatus Co. Ltd., China) at corresponding wavelength of 660nm which correspond to the maximum absorbance of were mixed and dissolved. The adsorption capacity for MB and their removal rate were calculated through Eqs. (1) and (2).

$$Q_e = \frac{(C_0 - C_e)V}{m} \tag{1}$$

$$\eta = \frac{C_0 - C_e}{C_0} \tag{2}$$

The values C_0 and C_e represent the initial and equilibrium concentration of MB (mg/L), V is the volume of solution (L), and m (g) is the mass of the adsorbent.

3. Results and discussion

3.1 Characterization

The FT-IR spectra of NS, CMNS, CMNS/AA composite were given in Fig. 1. The band at 3404 cm^{-1}, 2929 cm^{-1} and 1327 cm^{-1} could be associated with a stretching vibration caused by -OH, C-H and C-H bending vibration in the glucose unit, respectively (Wang *et al*. 2023). After the carboxymethylation and grafting polymerization, the absorption bands became narrower and shifted to higher wavenumbers. 1636 cm^{-1} is associated with H-O bending vibration, 1153 cm^{-1} and 1081 cm^{-1} corresponding to C-O-C stretching, 1019 cm^{-1} and 576 cm^{-1} are associated with glycosidic bond vibration (Eltaweil

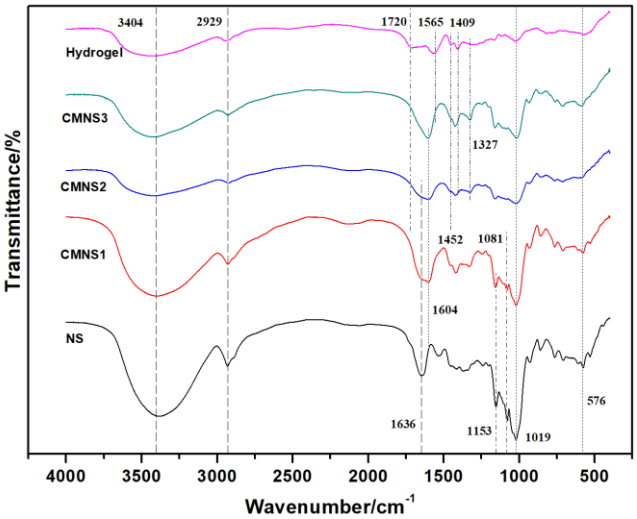

Fig. 1 FT-IR analysis of NS, CMNS1, CMNS2, CMNS3, and CMNS1/AA hydrogel

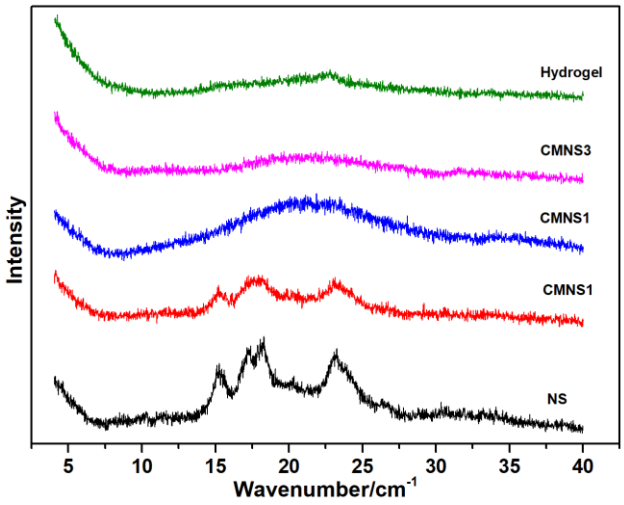

Fig. 2 XRD study of NS, CMNS1, CMNS2, CMNS3, and CMNS1/AA hydrogel

et al. 2020). A new absorption peak at 1604 cm^{-1} appeared in CMNS, which attributed to new C=O symmetry stretching vibration, confirming that the starch was etherified in the etherification process. The intensity of absorption band enhanced with the increase of the DS of CMNS. After grafting polymerization, the skeleton vibration peak of glucose ring was further weakened, and a new peak around 1720 cm^{-1}, was observed in Hydrogel which was related to the stretching vibration of the C=O bond (Meng *et al*. 2020). Meanwhile, three independent new characteristic peaks at 1565 cm^{-1}, 1452 cm^{-1}, and 1409 cm^{-1} were observed, which can be corresponding to the deformation vibration of N-H, symmetric tensile vibrations of COO^- and stretching vibration of C-N, respectively. The appearance of these new peaks indicates the presence of carbonyl, imide, and carboxyl groups in the hydrogel structure.

The NS, CMNS, and CMNS/AA composite XRD patterns were shown in Fig. 2. The NS was found to be a typical A-type crystalline, with strong diffraction peaks at

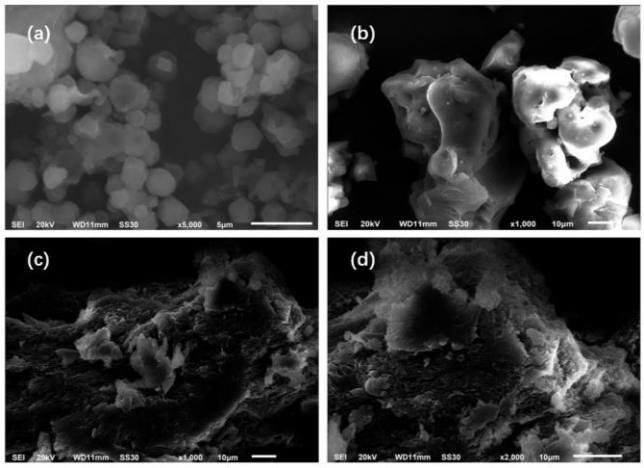

Fig. 3 SEM images of NS, CMNS1, and CMNS1/AA hydrogel

15.1°, 17.2°, 18.2°, and 23.2°, a weak peak at 20.3°. Similar patterns were also observed after carboxymethylation, and the intensity of the diffraction peak decreased with the increase of DS. When the DS above 0.571, the X-ray diffraction patterns of CMNS transferred to dispersion type, suggesting there was no the crystalline inside the granular. Meanwhile, after grafting of AA on the backbone of CMNS, the crystalline nature of the CMNS/AA hydrogel was disrupted and diminished, and it showed an amorphous nature with a smoother bump broad peak around from 10° to 30°. The breakdown of intra-molecular H-bonding could be one of the causes of the loss of crystalline nature. All the results above demonstrated the successful grafting copolymerization on the starch molecular chains.

The morphologies of NS, CMNS1, and CMNS1/AA hydrogel were observed, and the results were shown in Figure 3. NS has a regular appearance, and the surface morphologies of NS were spherical or polyhedral particles with a smooth surface. After the carboxymethylation, granules were disrupted to varying degrees, the granules were more irregular and slightly swollen, their surfaces became rough and wrinkled, and caves and holes could be observed on the surfaces of some granules. However, after graft-modification, i.e., grafting AA and NMBA on the backbone of CMNS, the shape of the molecules became rough and their surface area increased, and multiple connecting channels and open-pore structures can be observed in the image of Fig. 3(c) and 3(d). All of these would increase the surface area, which has more active sites and more favorable for adsorption.

3.2 Adsorption performance

The effects of different adsorbents such as HNS, HCMNS1, HCMNS2, and HCMNS3 on MB adsorption are illustrated in Fig. 4. It shows that the adsorption properties of etherified starch-based hydrogel are better than the native starch-based hydrogel. This may be due to initially the increase in CMNS and the increase in the number of carboxyl groups and hydroxyl groups in the composite adsorbent, so there are more adsorption sites to react with

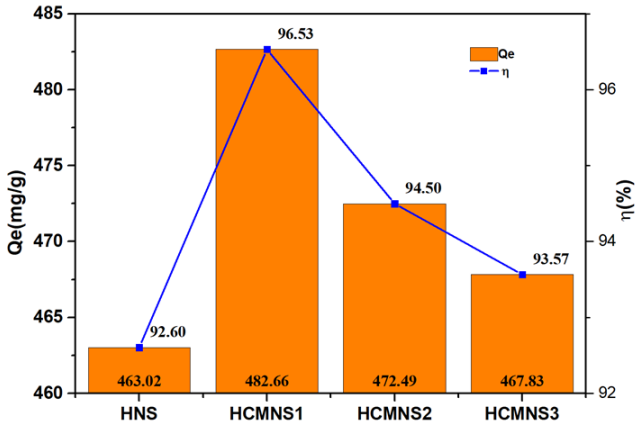

Fig. 4 The effect of adsorbents on adsorption of MB solution (100mg/L; 100mL; 298 K; 5h)

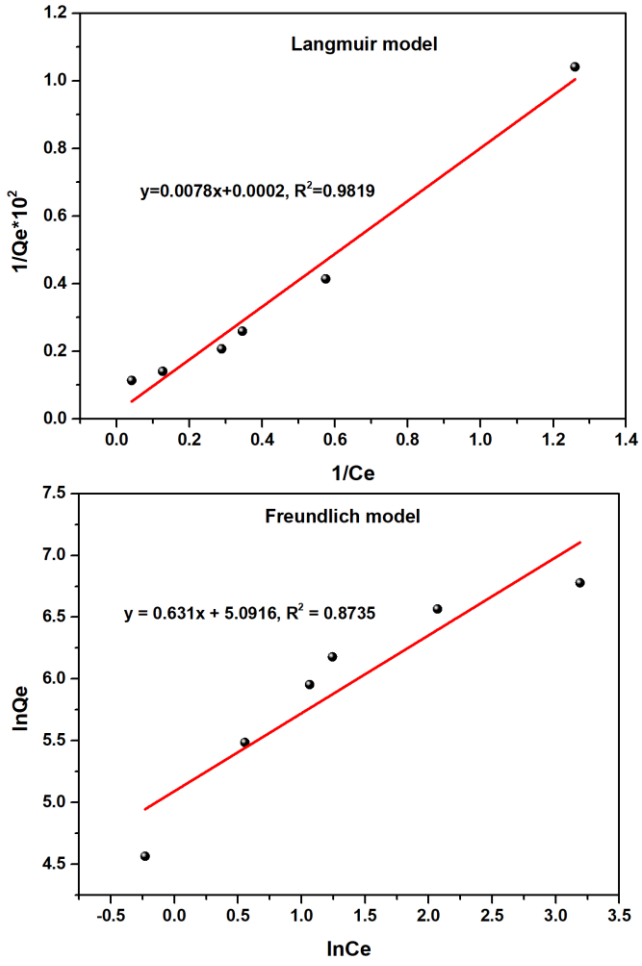

Fig. 5 The effect of initial concentration on adsorption of MB solution

Table 1 Isotherm parameters for MB adsorption

Model	Parameters		
Langmuir	K_F(L/mg)	Q_m(mg/g)	R^2
	0.0256	5000	0.9819
Freundlich	k_L(L/mg)	n_F	R^2
	162.65	1.585	0.8735

the dye molecules. However, increasing the DS of CMNS from 0.129 to 0.749, the adsorption capacity decreased from 482.7mg/g to 467.8mg/g, and the probable reason for this phenomenon is that carboxymethylation reaction occupied the reactive site of graft copolymerization (Meimoun *et al.* 2018). So, the grafting efficiency was decreases with the increase of DS of CMNS, and the absorption efficiency of carboxylic acid groups is lower than the polarity groups by the graft polymerization when the DS above 0.129. Finally, the adsorbent of HCMNS1 was chosen to investigate the adsorption experiment.

Adsorption isotherms of MB were investigated in some different initial concentration of MB solutions. Here are two sorption isotherm models, Freundlich and Langmuir isotherm models, which were chosen to simulate and evaluate the relationship between the Qe and Ce in aqueous solution. The Freundlich model and Langmuir isotherm model can be presented as (3) and (4), respectively (Dai *et al.* 2021).

$$Q_e = K_F C_e^{\frac{1}{n}} \tag{3}$$

$$\frac{C_e}{Q_e} = \frac{1}{K_L q_m} + \frac{C_e}{q_m} \tag{4}$$

The isothermal parameters of MB were explored. As discovered in Table 1, the adsorption isotherm of the Langmuir model has higher fitting degrees at normal temperature, and the coefficient of determination (R^2 = 0.9819) in Langmuir model were closer to 1. Furthermore, the value of Freundlich index 1/n is less than 1, indicating a preferential adsorption process.

Contact time also plays an important role in adsorption process, it is essential to estimate the equilibrium contact time and to reflect the adsorption kinetics of an adsorbent. The effect of contact time on MB adsorption by HCMNS1 was investigated. Fig. 6 showed adsorption results obtained for the adsorbent, and the growth rate of capacity is fast during the first 30min, while the second slope is slow until reaching the equilibrium which was observed after 60 min. The increment of the adsorption capacity of MB in the first stage is due to the vacant sites that are electrostatically available and able to accommodate the adsorbate molecules. After the equilibrium state, due to the repulsive forces between the MB molecules and HCMNS1, the rest of active sites could not be occupied by the MB molecules.

To research the adsorption kinetics better, the kinetic experimental data were guided into the quasi-first order (Eq. (5)) and quasi-second order (Eq. (6)) kinetic models, and the Weber-Morris model (Eq. (7)) (Dai *et al.* 2021).

$$\lg(q_e - q_t) = \lg q_e - \frac{k_1 t}{2.303} \tag{5}$$

$$\frac{t}{q_t} = \frac{1}{k_2} \times \frac{1}{q_e^2} + \frac{t}{q_e} \tag{6}$$

$$q_t = k_3 t^{\frac{1}{2}} + C \tag{7}$$

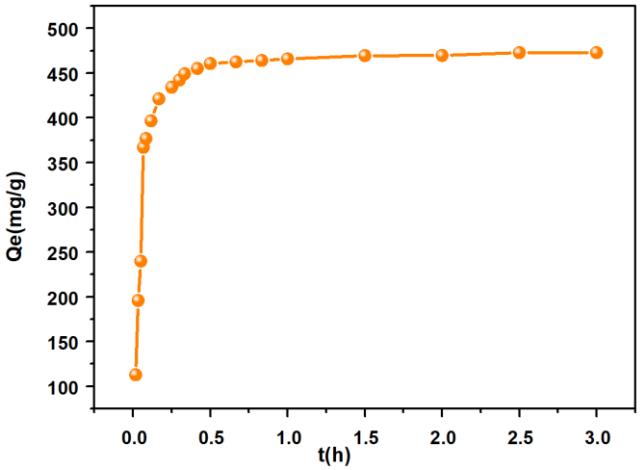

Fig. 6 The effect of contact time on adsorption of MB solution (100mg/L; 100mL; 298 K)

Thereinto, t (h), k_1 (h^{-1}), k_2 (g/(mg.h)) and k_3 (mg/g.$h^{1/2}$) are referred to as the contact time and the rate constants of quasi first-order, quasi second-order and diffusion kinetic models, respectively. Qe and q_t are the adsorption capacity (mg/g) of MB at equilibrium and corresponding time.

The obtained fitted plots and the kinetic parameters are displayed in Fig.7 and Table 2. Compared to Quasi-first-order model and Weber-Morris model, correlation coefficient for the Quasi-second order kinetic model is higher, and close to 1 unlimitedly. In addition, the calculated value of adsorbed quantities of MB is closer to the experimental data at corresponding temperature. Consequently, the quasi second-order model provides a good explanation for the MB adsorption process by HCMNS1, and the adsorption of MB appeared to be controlled by the chemisorption process simultaneously (Dai *et al*. 2021). Moreover, to identify the diffusion mechanism, the intraparticle diffusion model was used, and the plots of Qt to $t^{1/2}$ was illustrated in Fig.7 which give three linear lines for MB adsorption. According to Weber and Morris, the adsorption of MB on the surface of CMNS-based composite hydrogel occurs in three stages. The parameters calculated from these linear plots are summarized in Table 2. It is noticed that the fitting curve does not pass through the origin which indicating that the adsorption process is also jointly controlled by other adsorption stages, not just intraparticle diffusion (Roosen *et al*. 2017). As shown in Fig. 7 and Table 2, the first linearity represents the step of rapid adsorption or adsorption on the external surface. This is mainly a concern with hydrogen bonding and electrostatic interaction between carboxyl groups, hydroxyl groups and MB molecules. The second stage is belonged to the delayed diffusion of the MB dye molecules. The third stage declares the attainment of equilibrium. Moreover, it can be seen clearly from the intra-particle plot that the slopes of the three stages are in the order: first stage > second stage > third stage, and the intercept values present an opposite trend. All these reflected that the adsorption of MB on composite hydrogel may be complex and consist of surface adsorption and intraparticle diffusion (Eltaweil *et al*. 2020).

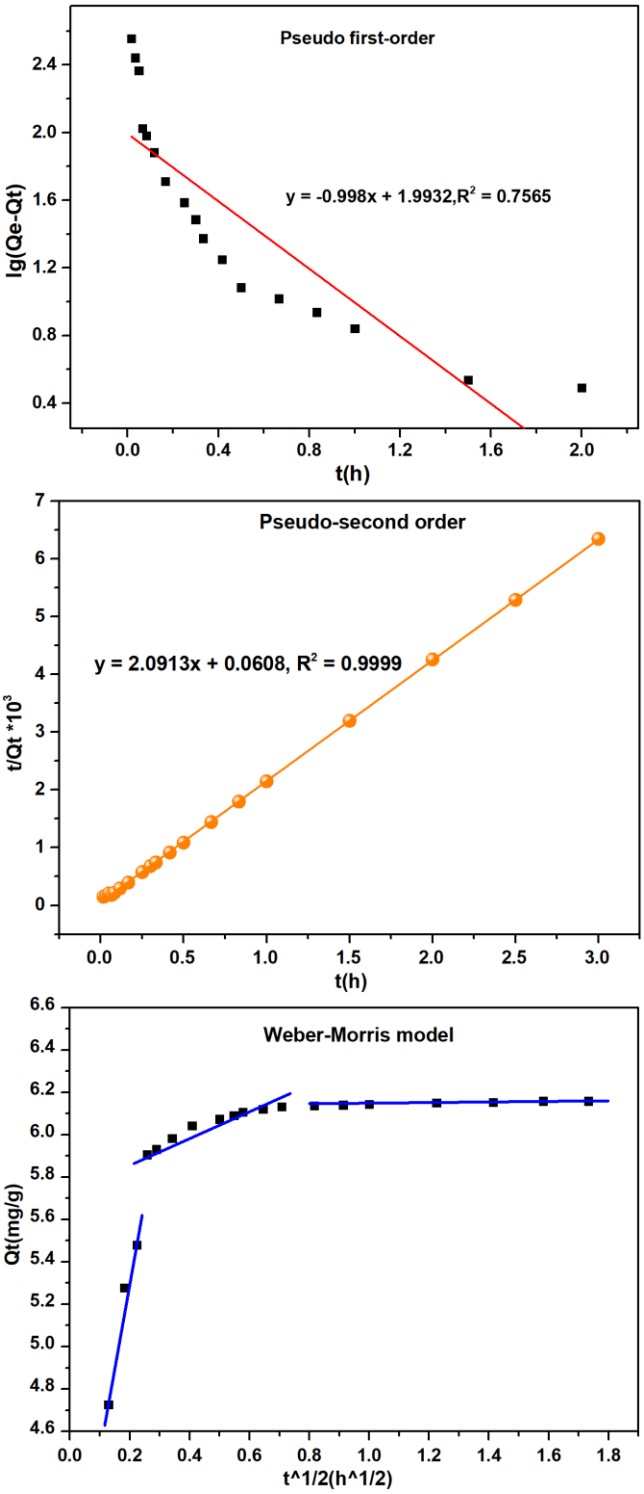

Fig. 7 Kinetics model curves of MB in water adsorption onto the HCMNS1 (100mg/L; 100mL; 298 K)

4. Conclusions

The Euryale ferox starch was successfully extracted by ethanol-alkali extraction, the etherified starches were successfully synthesized. Meanwhile, the etherified starch-based graft copolymerization composite hydrogels were prepared and their efficiency in the removal of MB were investigated. Moreover, the adsorption capacity can be

Table 2 Kinetic parameters for MB adsorption

Model		Parameters		
Quasi-first order		$k_1(h^{-1})$	Qe/(mg/g)[a]	R^2
		2.298	98.45	0.7565
Quasi-second order		k_2/(g/mg.h)	Qe/(mg/g)[a]	R^2
		0.2286	478.17	0.9999
Weber-Morris		k_3/(mg/g.$h^{1/2}$)	C	R^2
	Step1	8.0956	3.3717	0.9662
	Step2	0.5092	5.8014	0.9333
	Step3	0.0246	6.1182	0.9531

[a)] Qe is the adsorption quantity of the calculative value; the experimental values of Qe at 298K is 472.8mg/g

improved further by carboxymethylation, the rising tendency decreases with the increase of the DS of CMNS. Data obtained clarified that the adsorption of MB on the surface of the adsorbent composite is more fitted to Langmuir isotherm than Freundlich isotherm. The Maximum Qe is 472.5 mg/g and the adsorption process follows the pseudo-second order kinetic model. From this, we can say that the low cost, biodegradable and environmentally friendly nature of Euryale ferox starch-based hydrogel would make it the most favorable candidate in water purification technology.

Acknowledgments

We wish to acknowledge the financial support from the University Natural Science Research Key Project of Anhui Province (2023AH051619), Post-doctoral Program of Anhui Province (2020B406), Clinical Research Project of Anhui University of Chinese Medicine (LAQN007), and Industry-University-Research Projects (HX2020188), Innovaton and Entrepreneurship Training Program for College Students of Chuzhou University (2023CXXL103, 2024CXXL20501).

References

Bhat M.S. and Arya S.S. (2023), "Esterified unpopped foxnut (Euryale ferox) starch: molecular and rheological characterization", *J. Sci. Food Agric*., **103**, 2492-2501. https://doi.org/10.1002/jsfa.12440

Biswas P., Das M., Boral S., Mukherjee G., Chaudhury K. and Banerjee R. (2020), "Enzyme mediated resistant starch production from Indian Fox Nut (Euryale ferox) and studies on digestibility and functional properties", *Carbohyd. Polym.*, **237**, 116158. https://doi.org/10.1016/j.carbpol.2020.116158

Chen Y., Liu H., Xia M.S., Cao M.M., Nie Z.G. and Gao J.K. (2022), "Green multifunctional PVA composite hydrogel-membrance for the efficient purification of emulsified oil wastewater containing Pb^{2+} ions", *Sci. Total Environ.*, **856**, 159721. https://doi.org/10.1016/j.scitotenv.2022.159271

Dai K., Zhang J., Kou J.W., Yang P.P., Li M., Tang C.L., Zhuang W., Ying H.J. and Wu J.L., (2021), "Tunable synthesis of polyethylene polyamine modified lignin and application for efficient adsorption of Fe^{2+} in super acid system", *Sep. Purif. Technol*., **272**, 118950. https://doi.org/10.1016/j.seppur.2021.118950

Devi M. B. and Deka S.C. (2022), "Physicochemical properties, and structure of starches of foxnut (Euryale ferox Salisb.) from India and its application", *J Food Proc. Preserv*., **46**, e16262. https://doi.org/10.1111/jfpp.16262

Eltaweil A.S., Elgarhy G.S., El-Subruiti G. and Omer A.M. (2020), "Carboxymethyl cellulose/ carboxylated graphene oxide composite microbeads for efficient adsorption of cationic methylene blue dye", *Int. J Biol. Macromol*., **154**, 307-318. https://doi.org/10.1016/j.ijbiomac.2020.03.122

Guo Y.H., Bae J., Fang Z.W., Li P.P., Zhao F. and Yu G.H. (2020), "Hydrogels and Hydrogel-derived materials for energy and water sustainability", *Chem. Rev.*, **120**, 7642-7707. https://doi.org/10.1021/acs.chemrev.0c00345

Huang, H.H., Jiang, Q.Q., Chen, Y.L., Li, X., Mao, X.H., Chen, X.T., Huang, L.Q. and Gao, W.Y. (2016), "Preparation, physico–chemical characterization and biological activities of two modified starches from yam (Dioscorea Opposita Thunb.)", *Food Hydrocolloids*, **55**, 244-253. https://doi.org/10.1016/j.foodhyd.2015.11.016

Jha, V., Shalini, R., Kumari, A., Jha, P. and Sah N.K. (2018), "Aquacultural, nutritional and therapeutic biology of delicious seeds of euryale ferox salisb.: A minireview", *Curr. Pharm. Biotech*., **19**, 545-555. https://doi.org/10.2174/1389201019666180808160058

Jiang, J., Ou, H., Chen, R., Lu H., Zhou, L. and Yang, Z. (2023), "The ethnopharmacological, phytochemical, and pharmacological review of *Euryale ferox* Salisb.: A chinese medicine food homology", *Molecules*, **28**, 4399. https://doi.org/10.3390/molecules28114399

Khadatkar A., Mehta C.R. and Gite L.P. (2020), "Makhana (Euryle ferox Salisb.): A high-valued aquatic food crop with emphasis on its agronomic management-A review", *Scientia Horticulturae*., **261**, 108995. https://doi.org/10.1016/j.scienta.2019.108995

Maibam B.D., Nickhil C. and Deka S.C. (2023), "Preparation, physicochemical characterization, and in vitro starch digestibility on complex of Euryale ferox kernel starch with ferulic acid and quercetin", *Int. J Biol. Macromol*., **250**, 126178. https://doi.org/10.1016/j.ijbiomac.2023.126178

Musarurwa, H. and Tavengwa, N.T. (2020), "Application of carboxymethyl polysaccharides as bio-sorbents for the sequestration of heavy metals in aquatic environments", *Carbohyd Polym*., **237**, 116142. https://doi.org/10.1016/j.carbpol.2020.116142

Meimoun J., Wiatz V., Saint-Loup R., Parcq J., Favrelle A., Bonnet F. and Zinck P. (2018), "Modification of starch by graft copolymerization", *Starch*, **70**, 1600351. https://doi.org/10.1002/star.201600351

Meng R., Wu Z.Z., Xie H.Q., Xu G.X., Cheng J.S. and Zhang B.

(2020), "Preparation, characterization, and encapsulation capability of the hydrogel cross-linked by esterified tapioca starch", *Int. J Biol. Macromol*., **155**, 1-5. https://doi.org/10.1016/j.ijbiomac.2020.03.141

Roosen J., Mullens S. and Binnemans K. (2017), "Multifunctional Alginate–Sulfonate–Silica Sphere-Shaped Adsorbent Particles for the Recovery of Indium (III) from Secondary Resources", *Ind. Eng. Chem. Res*., **56**, 8677-8688. https://doi.org/10.1021/acs.iecr.7b01101

Shweta, K.Y. and Saxena D.C. (2021), "Valorization of unpopped Foxnut starch in stabilizing Pickering emulsion using OSA modification", *Int. J Biol. Macromol*., **191**, 657-667. https://doi.org/10.1016/j.ijbiomac.2021.09.148

Wang Q., Liu L.C., Huang Z.H., Bao K., Jing Z.H. and Wu Q.N. (2023), "Structure, and physicochemical properties of low digestible Euryale ferox Salisb. seed starch", *J. Sci. Food Agric*., **103**, 3850-3859. https://doi.org/10.1002/jsfa.12299

Wilpiszewska, K., Antosik, A.K. and Spychaj, T. (2015), "Novel hydrophilic carboxymethyl starch/montmorillonite nano-composite films", *Carbohyd. Polym*., **128**, 82-89. http://doi.org/10.1016/j.carbpol.2015.04.023

Yang, Y.X., Chen, Q., Yu, A.Z., Tong, S. and Gu, Z.Y. (2021), "Study on structural characterization, physicochemical properties, and digestive properties of Euryale ferox resistant starch", *Food Chem*., **359**, 129924. https://doi.org/10.1016/j.foodchem.2021.129924

Zdanowicz M. Spychaj T. and Lendzion-Bieluń Z. (2014), "Crosslinked carboxymethyl starch: One step synthesis and sorption characteristics", *Int. J Biol. Macromol*., **71**, 87-93. https://doi.org/10.1016/j.ijbiomac.2014.04.043

Zhang L., Zeng J.C., Yuan E., Chen J.G., Zhang Q.F., Wang Z.D. and Yin Z.P. (2023), "Extraction, identification, and starch-digestion inhibition of phenolics from Euryale ferox seed coat", *J. Sci. Food Agric*., **103**, 3437-3446. https://doi.org/10.1002/jsfa.12460

Zhao L., Chen Y.Q., Zeng J.C., Zang J.W., Liang Q., Tang D.B., Wang Z.D. and Yin Z.P. (2022), "Digestive and physico-chemical properties of small granular starch from euryale ferox seeds growing in Yugan of China", *Food Biophys*., **17**, 126-135. https://doi.org/10.1007/s11483-021-09706-7

Zia-ud-Din, Xiong H.G. and Peng F. (2015), "Physical and chemical modification of starches: A review", *Crit. Rev. Food Sci*. **57**, 2691-2705. http://doi.org/10.1080/10408398.2015.1087379